Ice flow dynamics and mass loss of Totten Glacier, East Antarctica from 1989 to 2015

Xin Li[1], Eric Rignot[1,2], Jeremie Mouginot[1], and Bernd Scheuchl[1]

Corresponding author: Xin Li, Department of Earth System Science, University of California Irvine, Irvine, CA 92697-3100, USA. (xin.li@uci.edu)

[1] Dept. of Earth System Science,

University of California, Irvine Irvine, CA,

USA

[2] Jet Propulsion Laboratory, California

Institute of Technology Pasadena, CA, USA

This article has been accepted for publication and undergone full peer review but has not been through the copyediting, typesetting, pagination and proofreading process, which may lead to differences between this version and the Version of Record. Please cite this article as doi: 10.1002/2016GL069173

Totten Glacier has the largest ice discharge in East Antarctica and a basin grounded mostly below sea level. Satellite altimetry data have revealed ice thinning in areas of fast flow. Here, we present a time series of ice velocity measurements spanning from 1989 to 2015 using Landsat and interferometric synthetic-aperture radar data, combined with ice thickness from Operation IceBridge, and surface mass balance from RACMO2.3. We find that the glacier speed exceeded its balance speed in 1989-1996, slowed down by 11±12% in 2000 to bring its ice flux in balance with accumulation (65±4 Gt/yr), then accelerated by 18±3% until 2007, and remained constant thereafter. The average ice mass loss (7±2 Gt/yr) is dominated by ice dynamics (73%). Its acceleration (0.6±0.3 Gt/yr^2) is dominated by surface mass balance (80%). Ice velocity apparently increased when ocean temperature was warmer, which suggests a linkage between ice dynamics and ocean temperature.

1. Introduction

Totten Glacier has the largest ice discharge in East Antarctica. Its ice flux into the southern ocean was about 71±3 Gt/yr in 2003-2008 [*Rignot et al.*, 2013]. Most of its drainage basin is grounded well below sea level [*Young et al.*, 2011]. If all ice contained in its basin were to melt into the ocean, the glacier would raise global sea level by 3.9 m [*Li et al.*, 2015]. Oceanographic data are few in this part of Antarctica but existing data indicate the presence of warm modified Circumpolar Deep Water (mCDW) at about 0°C below 500 m depth on the continental shelf [*Bindoff et al.*, 2000; *Williams et al.*, 2011]. The bathymetry beneath and in front of its 130-km long ice shelf holds potential pathways for intrusion of this mCDW into the ice shelf cavity [*Greenbaum et al.*, 2015]. This would explain the high area-average ice shelf melt rate recorded on Totten Ice Shelf (10.5±0.7 m/yr) compared to other ice shelves in East Antarctica [*Rignot et al.*, 2013].

Examination of changes in ice surface elevation over time indicates ice-shelf thinning in 2003-2008 but no significant long-term trend for the time period 1994-2012 [*Paolo et al.*, 2015]. In contrast, the satellite radar altimetry record on land indicates that ice thinning took place in areas of fast flow, with little to no thinning in the surrounding, slower-moving areas [*Zwally et al.*, 2005; *Davis et al.*, 2005; *Shepherd and Wingham*, 2007; *Flament and Rémy*, 2012; *Horwath et al.*, 2012; *McMillan et al.*, 2014]. Ice thinning at the grounding line of the fastest portion of Totten Glacier averaged 1.7±0.2 m/yr for the period 2003-2008 with ICESat [*Pritchard et al.*, 2009, 2012] and 0.5±0.01 m/yr with Cryosat-2 for 2010-2013 [*McMillan et al.*, 2014]. Time-variable gravity data from the Gravity Recovery and Climate Experiment (GRACE) for the time period 2003-2013 suggest an accelerating

mass loss for Totten, Moscow University and Frost combined [*Velicogna et al.*, 2014; *Williams et al.*, 2014]. Comparison of the mass loss derived from GRACE with time series of surface mass balance (SMB) anomalies from the Regional Atmospheric Climate Model (RACMO2) [*Lenaerts et al.*, 2012] over the same time period suggests only 40% of the signal is explained by SMB [*Velicogna et al.*, 2014].

A recent analysis showed that the glacier grounding line retreated by 1 to 3 km between 1996 and 2013, corresponding to an average ice thinning rate of 0.7±0.1 m/yr [*Li et al.*, 2015]. This magnitude thinning is consistent with the altimetry record and suggests that ice has been flowing faster than the speed required to maintain a state of mass balance with snowfall in the interior region. A broad area of grounded ice only a few tens of meters above hydrostatic equilibrium, or ice plain, was also found immediately upstream of the present-day grounding line, which implies that only a small change in ice thickness could have a large impact on the glacier flow because large areas of ice could become easily ungrounded and reduce buttressing of upstream ice. Changes in ice velocity have, however, eluded observations.

Here, we present an extensive record of ice velocity for Totten Glacier from year 1989 to present using a suite of interferometric synthetic aperture radars (InSARs) and Landsat data. We analyze the temporal variability of the ice velocity signal, the corresponding fluctuations in ice discharge using ice thickness data from Operation IceBridge (OIB) [*Blankenship et al.*, 2011, updated 2013], and compare the results with RACMO2.3 SMB products [*van Wessem et al.*, 2014] to determine the long-term trend mass balance of the glacier and the exact partitioning of the mass loss between surface mass balance processes

and ice dynamics. We discuss how this evolution may relate to ocean conditions in front of Totten Glacier and how the glacier may change with warmer ocean temperature.

2. Data and Methods

To measure ice surface velocity, we use optical and InSAR data from a set of satellite platforms that include the US Landsat MultiSpectral Scanner (Landsat-4), Enhanced Thematic Mapper Plus (Landsat-7), and Operational Land Imager (Landsat-8), the European Earth Remote Sensing imaging radar satellite (ERS-1/2), the Canadian RADARSAT-1 and RADARSAT-2 radar, the Japanese Advanced Land Observation System (ALOS) Phased-array L-band Synthetic Aperture Radar (PALSAR), the German TanDEM/TerraSAR-X (TDX/TSX), and the Italian COSMO-Skymed (CSK) constellation satellites. Our data collection spans year 1989 to 2015 and represents the most comprehensive list of observations assembled to date in this area (Table S1).

The Totten Glacier sector is challenging to study with remote sensing because of heavy precipitation by East Antarctic standards and persistent katabatic winds which limit data quality for optical sensors and reduce coherence of the InSAR signal. An additional difficulty for ice velocity mapping is the absence of easily-recognizable points of known (typically zero) ice velocity in the proximity of the glacier. While Law Dome is an obvious reference, high snowfall accumulation along its flanks [*Goodwin*, 1990] limits the signal-to-noise ratio of the SAR data and reduces phase coherence because of its low radar backscatter cross section. Points with near-zero velocity at the coast only include a few small ice rises [*Rignot et al.*, 2011]. The glacier is flanked by Moscow University Ice Shelf to the east, with its own flow regime and a similar lack of reliable reference velocity points.

This configuration requires the mapping to be extended to the ice divides of the glaciers (zero velocity) in order to calibrate the data, i.e. several hundreds km from the glacier grounding line [*Mouginot et al.*, 2012]. The Totten basin is also close to the south magnetic pole so that InSAR data are affected by above-average ionospheric noise [*Mouginot et al.*, 2012]. To detect small changes in ice velocity of the glacier, these factors need to be carefully weighed to obtain the highest quality velocity products.

Ice surface velocities in 1989 and 2001 are derived semi-automatically from Landsat-4 band 3 and Landsat-7 band 8 (panchromatic) data to achieve the best contrast and spatial resolution. We geo-reference sequential images of Landsat data to a Landsat-8 image with the same path/row using ground control points (GCPs) of near-zero velocity from the Antarctic-wide velocity map [*Rignot et al.*, 2011]. We estimate a registration accuracy of better than 1 pixel (30 m for Landsat-4, 15 m for Landsat-7). Small scale ($<$ 5 pixels) ice surface features such as crevasses and rifts are identified and tracked on pairs of registered images. The two-dimensional displacements are converted into velocity flow vectors (Figure S1). We estimate an accuracy of 2 pixels for the measured displacements, which translates into an error in velocity of 98 m/yr for Landsat-4 data in 1989 and 10 m/yr for Landsat-7 data in 2001.

We have high phase coherence from ERS-1/2 1996 1-day repeat cycle SAR data and derive the line-of-sight (across-track) velocity component [*Goldstein et al.*, 1993]. Tidal signals on the ice shelf are removed using products from CATS2008a_opt tide model [*Padman et al.*, 2008] and the TPXO6.2 load model [*Egbert and Erofeeva*, 2002] following *Scheuchl et al.* [2012], but this does not affect the grounded ice velocity. No ascending

passes exist in the area. We therefore use a multiple aperture interferometry (MAI) technique [*Bechor and Zebker*, 2006] to derive the along-track velocity component. In total, we estimate an error of 49 m/yr in speed dominated by ionospheric errors.

The remaining InSAR data are processed using a speckle tracking algorithm [*Michel and Rignot*, 1999] using data from *Rignot et al.* [2011] for the time period 2007-2009, combined with the following new data: RADARSAT-1 24-day repeat data from year 2000, ERS-1 35-day repeat data from 2005, ALOS PALSAR 46-day repeat data for five consecutive years in 2006-2010, TDX/TSX 11-day repeat data from 2011, and RADARSAT-2 24-day repeat data from 2015. We have multiple datasets in 2013: 11-day repeat TDX/TSX data, 3-day repeat CSK data, and 48-day repeat Landsat-8 data. For ice motion product calibration, we use the processing chain of *Mouginot et al.* [2012]. We use long tracks spanning the entire drainage basin to calibrate the data at the ice divides (Figure S2). The estimated errors range from 10 m/yr to 17 m/yr depending on the sensor repeat cycle and its operating frequency. Ice motion products from Landsat-8 data are derived using a cross-correlation algorithm similar to that used for InSAR data. Figure S3 shows the velocity maps for each year.

Ice velocities are combined with ice thickness from OIB [*Blankenship et al.*, 2011, updated 2013] from the time period 2009-2012 [*Blankenship et al.*, 2011, updated 2013] to calculate the ice flux as in *Mouginot et al.* [2014]. We estimate the ice flux along the interferometrically-derived 2013 grounding line (Figure 1a, yellow line) [*Li et al.*, 2015] and along OIB ice thickness profiles (Figure 1a, orange line) with correction for SMB in between to obtain ice fluxes equivalent to that measured at the 2013 grounding line.

When the velocity measurements have gaps, e.g. in years 1989, 2001, 2005 and 2015, we calculate a scaling factor in reference to the most complete velocity mapping (year 2007) to scale the ice flux accordingly (Supplementary Material). We estimate the errors in ice discharge using multiple flux gates as in *Mouginot et al.* [2014] (Table S2). Temporal changes in ice thickness are not included in the calculation because they remain small (1 m/yr) compared to ice thickness (2 km).

SMB values are integrated over the drainage basin of Totten determined from digital elevation data and ice flow vectors [*Rignot et al.*, 2013]. The bias in SMB in East Antarctica has been estimated to range from 3 to 16% depending on elevation [*van Wessem et al.*, 2014]. We calculate an elevation-weighted average uncertainty of 4.1 Gt/yr for the Totten basin (see Supplementary Material). We use the mean SMB for the time period 1979-2014 as a reference for the long-term average SMB and compare it with ice discharge to estimate the long-term glacier mass balance. We also calculate the cumulative mass balance since 1989 using the time series of differences between SMB and ice discharge. The mean mass balance and change in mass balance are calculated using a weighted least square regression following *Sutterley et al.* [2014]. We use the Akaike Information Criterion for finite sample sizes (AIC_c) [*Burnham and Anderson*, 2002] to select the order of the regression model to fit the cumulative mass anomaly.

To compare our results with climate forcing, we examine the air temperature record at Casey Station, about 190 km to the west of Totten [*Turner et al.*, 2004]. We find no trend in air temperature at Casey Station during the time period (Figure S4). We also extract ocean temperatures from the Estimating the Circulation and Climate of the Ocean, Phase

II (ECCO2) solution [*Menemenlis et al.*, 2008] averaged over a spatial domain covering 115^o E to 118^o E and 65.5^o S and 67^o S. ECCO2 is a data assimilation analysis that combines a general circulation model (MITgcm) with a variety of observational data mostly off the continental shelf. We calculate the average potential temperature between 400 and 650 m depth as this corresponds to the observed depth of mCDW [*Williams et al.*, 2011]. We also examine temperature data from two other reconstructions: (1) ECCO_v4 [*Forget et al.*, 2015] and (2) Southern Ocean State Estimation (SOSE) [*Mazloff et al.*, 2010] over shorter time periods to compare various reconstructions of ocean temperature in this part of the Southern Ocean (Figure S5).

3. Results

Figure 1 shows the magnitude of the surface velocity and flow direction of Totten Glacier. The pattern of fast flow (> 50 m/yr) initiates in the deep Aurora Subglacial Basin, about 350 km from the coast. The ice flow is diverted into two tributaries along the flanks of Law Dome, one towards Vanderford Glacier into the Vincennes Bay to the west and the other toward Totten on the east. The main stream of Totten carries most of the ice and flows down a confined, 25-km wide ice shelf at a speed of 800 m/yr, which is a typical value in East Antarctica [*Rignot et al.*, 2011], but a low value compared to ice shelves in the Amundsen Sea sector of West Antarctica [*Mouginot et al.*, 2014]. On the broad eastern side of its grounding line, a tributary initiates 190 km inland and merges into the main stream at a speed of 430 m/yr. At the ice front, the ice shelf flows at 1,800 m/yr and calves off with an iceberg production of 28±2 Gt/yr in 2003-2008 [*Rignot et al.*, 2013].

At the grounding line of the main stream of Totten Glacier (box A in Figure 1), we find that the ice speed decreased by 86±98 m/yr, or 11±12% during the time period 1989-2000. The glacier speed then increased by 120±21 m/yr, or 18±3%, to peak around 2007 (Figure 2a). Since 2007, the glacier speed has remained constant, with a slight decrease of 30±20 m/yr, or 4±3% in 7 years. These changes in ice speed are reflected on the ice shelf, almost in linear agreement with those recorded on grounded ice.

As shown in Figure 3, most changes in speed, on both grounded and floating ice, are concentrated in the immediate vicinity of the grounding line, along the faster portion of the glacier or main stream. From 2007 to 2013, the change in ice speed extended 8 km upstream from the grounding line. The inland portion of the drainage system has for the most part remained unchanged. At the eastern tributary (box B in Figure 1), we detect a similar pattern of velocity change, but with a much smaller magnitude (Figure 2a). At this location, the variability in flow speed is within 50 m/yr, close to our measurement noise. Overall, there is no significant trend in velocity along the eastern tributary, i.e. most of the detected changes in speed are concentrated along the main stream of the glacier.

The calculated ice discharge is higher than the reference SMB of 65±4 Gt/yr for the period 1989-2014 (Figure 2c), suggesting that the glacier has been flowing faster than its equilibrium speed for 26 years. The exception is year 2000, when the glacier was flowing at its lowest speed and the ice discharge was within error bars of the balance discharge.

The cumulative glacier mass balance (Figure 2d) is significantly modulated by variations in SMB. On average, we calculate a mass loss dM/dt of 6.8±2.4 Gt/yr. The cumulative

mass anomaly displays a quadratic decreasing trend at a statistically significant level with an acceleration (d^2M/dt^2) of -0.6±0.3 Gt/yr^2. 80% of the acceleration signal is due to low SMB values during 2003-2014. In terms of total mass loss, 27±8% of the signal is due to SMB and 73±8% to ice dynamics. Hence, the glacier has been flowing at speeds above that required to maintain a state of mass balance for a long time, and the recent fluctuations in mass loss are mostly due to a variability in SMB.

Figure 2b shows a time series of continental-shelf ocean temperature in front of Totten Glacier. To compare the time series with the velocity data, we extract ocean temperature within each velocity data epoch (red dots). Reconstructed ocean temperature is warm in the 1990s, then cools to reach a minimum around year 2000. After 2000, ocean temperature increases to maintain high values during 2005-2009, then decreases in recent years. We fit a piecewise linear regression with breakpoints at 2000 and 2007 to extract trends during the observed acceleration/deceleration periods of the glacier (dashed line). Between 1992 and 2000, when ice flow slowed (80% confidence interval), the sub-surface ocean water on continental shelf cooled by 1.1°C. Between 2000 and 2007, when the glacier sped up, the ocean temperature increased by 0.6°C. Since 2007, the modeled ocean temperature has cooled by 1.2°C. We also examined solutions from ECCO_v4 (1992-2011) and SOSE (2005-2011). Both reconstructions show potential temperatures 0.6-0.9 °C warmer than ECCO2 in this region, but with a similar temporal trend (Figure S5). We end up using ECCO2 because it has the longest time span (1992-2013). We also find that the average potential temperature of -0.4±0.03 °C from ECCO2 is in better agreement with new *in situ* observations [*Zielinski et al.*, 2015; *Rintoul et al.*, 2015] compared to the other

two solutions. We note, however, that this reconstructed temperature cannot replace the need for actual temperature data.

4. Discussion

We find a reasonable agreement between the thinning reported by altimetry data and our mass budget results (Figure S6, Table S3). Thinning rates increased during periods of accelerated flow and decreased during periods of slow down. In terms of spatial patterns, most of the observed velocity change took place in the area of fast flow of Totten Glacier instead of its eastern tributary, which is consistent with the altimetry record [*Pritchard et al.*, 2009; *Flament and Rémy*, 2012]. From 1996 to 2013, the glacier speed increased by 10±5%, corresponding to a 1-3 km grounding line retreat [*Li et al.*, 2015]. The agreement between the thinning and speed up, together with the grounding line retreat, provides additional observational evidence for the dynamic thinning of Totten Glacier on top of the significant interannual variations in SMB.

We use the 1979-2014 average SMB to represent the long term glacier mass balance because ice core records from Law Dome show no long term trend in snow accumulation in the past 2,000 years [*van Ommen and Morgan*, 2010; *Roberts et al.*, 2015]. When comparing ice discharge with the reference SMB, we find the glacier was likely already flowing above equilibrium conditions in 1989 (73% confidence interval). Although the annual mass balance is affected by fluctuations in SMB, the overall glacier mass balance has been negative with high confidence. For the later part of the record, this conclusion is supported by GRACE [*Velicogna and Wahr*, 2013; *Velicogna et al.*, 2014], prior mass budget [*Rignot et al.*, 2008] and satellite altimetry studies. The estimated mass loss of

6.8±2.4 Gt/yr, or 10±3% of the ice flux, is compatible with independent studies (e.g. 4.6±0.5 Gt/yr [*Shepherd and Wingham*, 2007], 10±3 Gt/yr [*McMillan et al.*, 2014]). This mass loss is small compared to that experienced by glaciers in the Amundsen Sea sector in West Antarctica where the mass loss ranges from 30% to 40% of the balance ice flux [*Sutterley et al.*, 2014; *Mouginot et al.*, 2014]. Yet, the importance of the 10% imbalance of Totten Glacier is that the glacier holds a large potential for sea level rise and may be prone to rapid change if ice shelf melt rates were to change.

We attribute the changes in ice dynamics to oceanic forcing because field observations have shown the presence of mCDW on the continental shelf near Totten [*Bindoff et al.*, 2000; *Williams et al.*, 2011]. Warm mCDW fuels high melt rates in this area, and a change in ocean temperature is the most likely explanation for the observed change in ice dynamics. Sea floor bathymetry from gravity inversion reveals the presence of a valley crossing the main sill in front of the glacier that is deeper than the thermocline depth [*Blankenship et al.*, 2015]. This valley may allow access of warm modified Circumpolar Deep Water (mCDW) to the sub-ice-shelf cavity and induce rapid ice shelf melting. The main stream is grounded $>$ 2,300 m below sea level at the grounding line, which is the deepest part of the sub-ice-shelf cavity. Ice shelf melt rates are expected to be highest in this region due to the pressure dependence of the freezing point of seawater. Remote sensing observations have shown that the most intensive ice melt taking place in this part of the sub-ice-shelf cavity [*Rignot et al.*, 2013]. Grounding line retreat has also been observed [*Li et al.*, 2015]. The reanalysis temperature data from ECCO2 solution indicates three periods of warming/cooling of the sub-surface water (450-600 m depth) on

the continental shelf, which agree with periods of acceleration/deceleration of the glacier. If this is correct, this indicates a significant sensitivity of the glacier to ocean temperature, which is consistent with the presence of an ice plain in the grounding line region [*Li et al.*, 2015]. Coastal polynya activities can cause short-term variability in subglacial melt rates by modulating mCDW access into the sub-ice-shelf cavity [*Khazendar et al.*, 2013; *Gwyther et al.*, 2014]. In the future, enhanced intrusion of mCDW on the continental shelf from polar contraction [*Mayewski et al.*, 2013] could increase ocean temperature and contribute to more mass loss from Totten Glacier. We recommend the collection of ocean temperature data in this region to determine the evolution of mCDW near the glacier front and to examine the influence of ocean water on ice dynamics in more details.

5. Conclusions

We assembled a 26-year long time series of ice velocity measurements on Totten Glacier to conclude that the glacier speed has fluctuated up to 18% during the time period, with low values around 2000, high values prior to 1996 and after 2002. In the last ten years, the glacier has maintained a relatively steady speed but has been flowing above equilibrium conditions. The glacier has been losing mass at a rate of 6.8±2.4 Gt/yr, or 10% of the total flux on average for the past 26 years. The main loss is caused by the speed up of the glacier along its main flow. Our results also suggests that the glacier may be strongly sensitive to ocean temperature. More detailed studies are needed to quantify the impact of ocean temperature on ice dynamics in this important sector of East Antarctica.

Acknowledgments. This work was performed at the University of California Irvine and at the California Institute of Technology's Jet Propulsion Laboratory, under Contracts

NNX13AN46G, NNX14AN03G, and NNX14AB93G with the Cryosphere Science Program of National Aeronautics and Space Administration. ERS-1/2 TanDEM data were provided by European Space Agency. TanDEM-X data were provided by German Aerospace Center (DLR), through Project XTI_GLAX0343. COSMO-SkyMed data ©ASI (2013) were provided by e-GEOS under ESA's TPM scheme (Category-1 Proposal ID 14871). We thank Dr. Benoit Legresy for providing the thinning rates.

References

Bechor, N. B. D., and H. A. Zebker, Measuring two-dimensional movements using a single InSAR pair, *Geophys. Res. Lett.*, *33*(16), 1–5, 2006.

Bindoff, N. L., M. A. Rosenberg, and M. J. Warner, On the circulation and water masses over the Antarctic continental slope and rise between 80 and 150°E, *Deep-Sea Res. Pt II*, *47*(12-13), 2299–2326, 2000.

Blankenship, D., et al., Increased ocean access to Totten Glacier, East Antarctica, in *AGU Fall Meeting Abstracts*, 2015.

Blankenship, D. D., S. D. Kempf, and D. A. Young, IceBridge HiCARS 1/2 L2 Geolocated Ice Thickness 2009-2012, *NASA DAAC at the NSIDC*, 2011, updated 2013.

Burnham, K. P., and D. R. Anderson, *Model Selection and Multimodel Inference*, 2nd ed. ed., Springer, New York, 2002.

Davis, C. H., Y. Li, J. R. McConnell, M. M. Frey, and E. Hanna, Snowfall-driven growth in East Antarctic ice sheet mitigates recent sea-level rise, *Science*, *308*(5730), 1898–1901, 2005.

Egbert, G. D., and S. Y. Erofeeva, Efficient inverse modeling of barotropic ocean tides, *J. Atmos. Ocean. Tech.*, *19*(2), 183–204, 2002.

Flament, T., and F. Rémy, Dynamic thinning of Antarctic glaciers from along-track repeat radar altimetry, *J. Glaciol.*, *58*(211), 830–840, 2012.

Forget, G., J.-M. Campin, P. Heimbach, C. N. Hill, R. M. Ponte, and C. Wunsch, ECCO version 4: an integrated framework for non-linear inverse modeling and global ocean state estimation, *Geosci. Model Dev.*, *8*(5), 3653–3743, 2015.

Fretwell, P., et al., Bedmap2: Improved ice bed, surface and thickness datasets for Antarctica, *The Cryosphere*, *7*, 375–393, 2013.

Goldstein, R. M., H. Engelhardt, B. Kamb, and R. M. Frolich, Satellite Radar Interferometry for Monitoring Ice Sheet Motion: Application to an Antarctic Ice Stream, *Science*, *262*(5139), 1525–1530, 1993.

Goodwin, I. D., Snow accumulation and surface topography in the katabatic zone of Eastern Wilkes Land, Antarctica, *Antarct. Sci.*, *2*(3), 235–242, 1990.

Greenbaum, J. S., et al., Ocean access to a cavity beneath Totten Glacier in East Antarctica, *Nat. Geosci.*, pp. 294–298, 2015.

Gwyther, D. E., B. K. Galton-Fenzi, J. R. Hunter, and J. L. Roberts, Simulated melt rates for the Totten and Dalton ice shelves, *Ocean Sci.*, *10*, 267–279, 2014.

Horwath, M., B. Legrésy, F. Rémy, F. Blarel, and J.-M. Lemoine, Consistent patterns of Antarctic ice sheet interannual variations from ENVISAT radar altimetry and GRACE satellite gravimetry, *Geophys. J. Int.*, *189*, 863,876, 2012.

Khazendar, A., M. P. Schodlok, I. Fenty, S. R. M. Ligtenberg, E. Rignot, and M. R. van den Broeke, Observed thinning of Totten Glacier is linked to coastal polynya variability, *Nat. Commun.*, *4*, 2857, 2013.

Lenaerts, J. T. M., M. van den Broeke, W. J. van de Berg, E. van Meijgaard, and P. K. Munneke, A new, high-resolution surface mass balance map of Antarctica (1979-2010) based on regional atmospheric climate modeling, *Geophys. Res. Lett.*, *39*, 1–5, 2012.

Li, X., E. Rignot, M. Morlighem, J. Mouginot, and B. Scheuchl, Grounding line retreat of Totten Glacier, East Antarctica, 1996 to 2013, *Geophys. Res. Lett.*, *42*, 8049–8056, 2015.

Mayewski, P. A., et al., West Antarctica's sensitivity to natural and human-forced climate change over the Holocene, *J. Quat. Sci.*, *28*, 40–48, 2013.

Mazloff, M. R., P. Heimbach, and C. Wunsch, An Eddy-Permitting Southern Ocean State Estimate, *J. Phys. Oceanogr.*, *40*, 880–899, 2010.

McMillan, M., A. Shepherd, A. Sundal, K. Briggs, A. Muir, A. Ridout, A. Hogg, and D. Wingham, Increased ice losses from Antarctica detected by CryoSat-2, *Geophys. Res. Lett.*, *41*, 3899–3905, 2014.

Menemenlis, D., J-M. Campin, P. Heimbach, C. Hill, T. Lee, A. Nguyen, M. Schodlok, and H. Zhang, ECCO2: High resolution global ocean and sea ice data synthesis, *Mercator Ocean Newsl.*, *31*, 13–21, 2008.

Michel, R., and E. Rignot, Flow of Glaciar Moreno, Argentina, from repeat-pass Shuttle Imaging Radar images: comparison of the phase correlation method with radar interferometry, *J. Glaciol.*, *45*(149), 93–100, 1999.

Mouginot, J., B. Scheuchl, E. Rignot, and R. Data, Mapping of Ice Motion in Antarctica Using Synthetic-Aperture Radar Data, *Remote Sens.*, *4*(9), 2753–2767, 2012.

Mouginot, J., E. Rignot, and B. Scheuchl, Sustained increase in ice discharge from the Amundsen Sea Embayment, West Antarctica, from 1973 to 2013, *Geophys. Res. Lett.*, *41*, 1576–1584, 2014.

Padman, L., S. Y. Erofeeva, and H. A. Fricker, Improving Antarctic tide models by assimilation of ICESat laser altimetry over ice shelves, *Geophys. Res. Lett.*, *35*(22), L22,504, 2008.

Paolo, F. S., H. A. Fricker, and L. Padman, Volume loss from Antarctic ice shelves is accelerating, *Science*, *348*(6232), 327–332, 2015.

Pritchard, H. D., R. J. Arthern, D. G. Vaughan, and L. A. Edwards, Extensive dynamic thinning on the margins of the Greenland and Antarctic ice sheets, *Nature*, *461*(7266), 971–5, 2009.

Pritchard, H. D., S. R. M. Ligtenberg, H. A. Fricker, D. G. Vaughan, M. R. van den Broeke, and L. Padman, Antarctic ice-sheet loss driven by basal melting of ice shelves, *Nature*, *484*(7395), 502–505, 2012.

Rignot, E., J. L. Bamber, M. van den Broeke, C. Davis, Y. Li, W. J. van de Berg, and E. van Meijgaard, Recent Antarctic ice mass loss from radarinterferometry and regional climatemodelling, *Nat. Geosci.*, *1*(2), 106–110, 2008.

Rignot, E., J. Mouginot, and B. Scheuchl, Ice flow of the Antarctic ice sheet., *Science*, *333*(August), 1427–1430, 2011.

Rignot, E., S. S. Jacobs, J. Mouginot, and B. Scheuchl, Ice Shelf Melting Around Antarctica, *Science*, (June), 1–6, 2013.

Rintoul, S., A. Orsi, A. Silvano, E. van Wijk, B. Pena-Molino, and M. Rosenberg, Direct evidence of warm water access to the Totten Glacier sub-ice shelf cavity, in *AGU Fall Meeting Abstracts*, 2015.

Roberts, J., C. Plummer, T. Vance, T. van Ommen, A. Moy, S. Poynter, A. Treverrow, M. Curran, and S. George, A two thousand year annual record of snow accumulation rates for Law Dome, East Antarctica, *Clim. Past*, *11*, 697–707, 2015.

Scambos, T., T. M. Haran, M. Fahnestock, T. H. Painter, and J. Bohlander, MODIS-based Mosaic of Antarctica (MOA) data sets: Continent-wide surface morphology and snow grain size, *Remote Sens. Environ.*, *111*(2-3), 242–257, 2007.

Scheuchl, B., J. Mouginot, and E. Rignot, Ice velocity changes in the Ross and Ronne sectors observed using satellite radar data from 1997 and 2009, *The Cryosphere*, *6*(5), 1019–1030, 2012.

Shepherd, A., and D. Wingham, Recent sea-level contributions of the Antarctic and Greenland ice sheets, *Science*, *315*(5818), 1529–32, 2007.

Sutterley, T. C., I. Velicogna, E. Rignot, J. Mouginot, T. Flament, M. R. van den Broeke, J. M. van Wessem, and C. H. Reijmer, Mass loss of the Amundsen Sea Embayment of West Antarctica from four independent techniques, *Geophys. Res. Lett.*, *41*(23), 8421–8428, 2014.

Turner, J., S. R. Colwell, G. J. Marshall, T. a. Lachlan-Cope, A. M. Carleton, P. D. Jones, V. Lagun, P. a. Reid, and S. Iagovkina, The SCAR READER project: Toward a

high-quality database of mean Antarctic meteorological observations, *J. Clim.*, *17*(14), 2890–2898, 2004.

van Ommen, T. D., and V. Morgan, Snowfall increase in coastal East Antarctica linked with southwest Western Australian drought, *Nat. Geosci.*, *3*(4), 267–272, 2010.

van Wessem, J. M., et al., Improved representation of East Antarctic surface mass balance in a regional atmospheric climate model, *J. Glaciol.*, *60*(222), 761–770, 2014.

Velicogna, I., and J. Wahr, Time-variable gravity observations of ice sheet mass balance: Precision and limitations of the GRACE satellite data, *Geophys. Res. Lett.*, *40*(12), 3055–3063, 2013.

Velicogna, I., T. C. Sutterley, and M. R. van den Broeke, Regional acceleration in ice mass loss from Greenland and Antarctica using GRACE time-variable gravity data, *Geophys. Res. Lett.*, *41*(22), 8130–8137, 2014.

Williams, G., A. J. S. Meijers, A. Poole, P. Mathiot, T. Tamura, and A. Klocker, Late winter oceanography off the Sabrina and BANZARE coast (117128E), East Antarctica, *Deep-Sea Res. Pt II*, *58*(9-10), 1194–1210, 2011.

Williams, S. D., P. Moore, M. a. King, and P. L. Whitehouse, Revisiting GRACE Antarctic ice mass trends and accelerations considering autocorrelation, *Earth Planet. Sci. Lett.*, *385*, 12–21, 2014.

Young, D. a., et al., A dynamic early East Antarctic Ice Sheet suggested by ice-covered fjord landscapes., *Nature*, *474*(7349), 72–75, 2011.

Zielinski, N., A. Orsi, and C. Webb, Currents and Transport across the eastern Sabrina Basin, East Antarctica, in *AGU Fall Meeting Abstracts*, 2015.

Zwally, J., M. B. Giovinetto, J. Li, H. G. Cornejo, M. a. Beckley, A. C. Brenner, J. L. Saba, and D. Yi, Mass changes of the Greenland and Antarctic ice sheets and shelves and contributions to sea-level rise: 1992-2002, *J. Glaciol.*, *51*(175), 509–527, 2005.

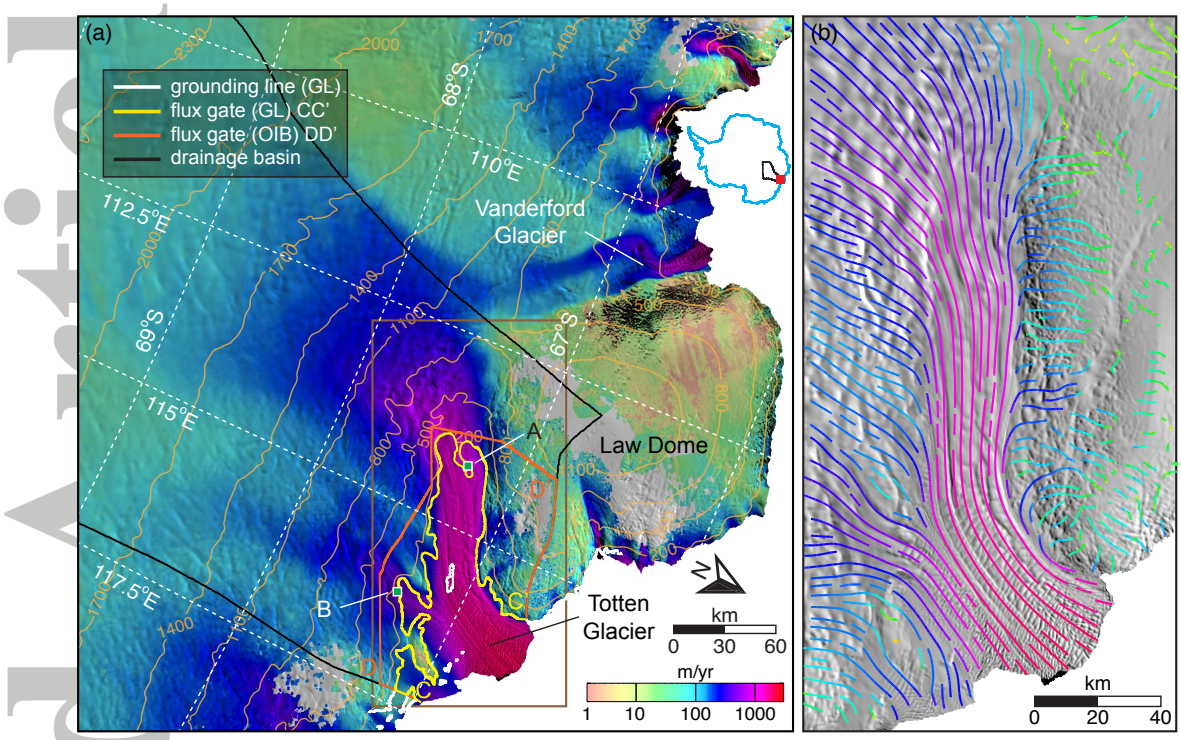

Figure 1. (a) Ice velocity magnitude and (b) direction of Totten Glacier, East Antarctica, color coded on a logarithmic scale and overlaid on MOA image [*Scambos et al.*, 2007] using ALOS PALSAR data from 2006-2010, and 2011 TDX/TSX, 2013 TDX/TSX, CSK and Landsat-8 data. The grounding line (GL) from 2013 is solid white. Flux gates are solid yellow (GL) and orange (along Operation IceBridge (OIB) ground tracks). Green boxes A and B delineate the area used to generate the velocity time series (Figure 2a). Brown box is the map outline of Figure 1b and 3. BEDMAP2 surface elevation [*Fretwell et al.*, 2013] contours are plotted at 300-m intervals.

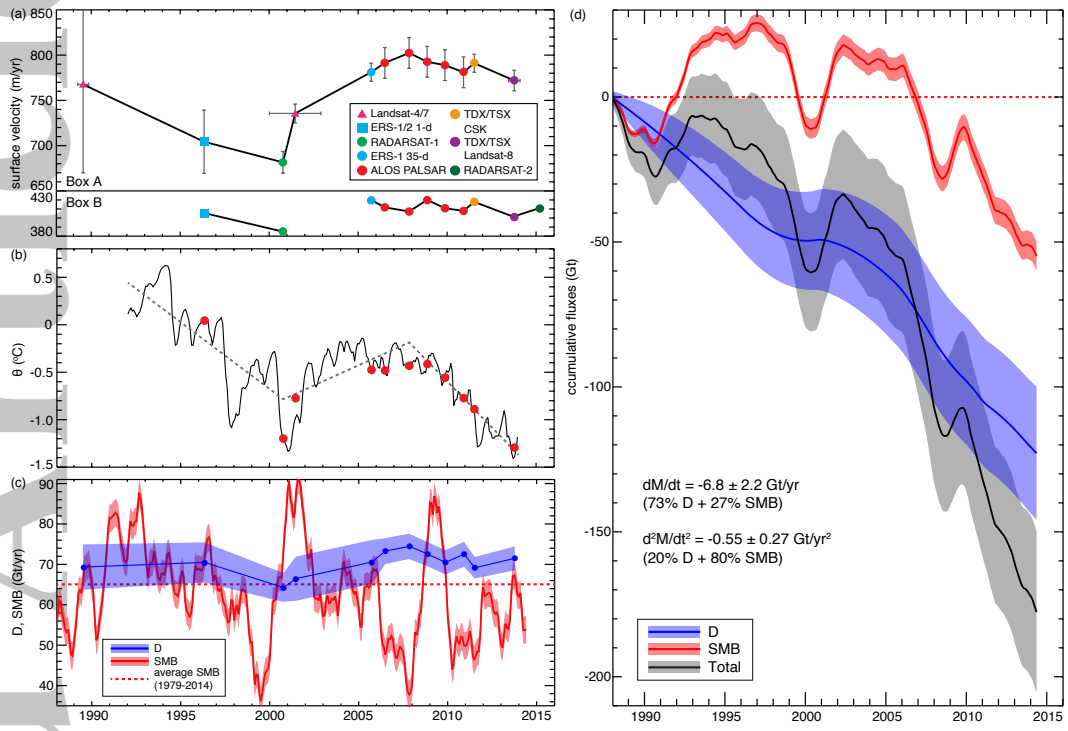

Figure 2. Time series of (a) ice velocity, (b) ice discharge (D) and surface mass balance (SMB), (c) sub-surface ocean potential temperature (450-600 m depth), and (d) cumulative mass anomalies on Totten Glacier, East Antarctica. (a) shows velocity change at the grounding line (box A on Figure 1), and at the east tributary (box B). Error bars for the bottom time series are the same as the top one. Red dots in (b) show average potential temperature for each velocity data epoch in (a). Grey dashed lines are fitted using a piecewise linear regression. SMB values in (c) are smoothed with a 12-month running filter. The total mass anomalies (black) in (d) are partitioned between the anomalies in SMB (red) and in ice discharge (D, in blue).

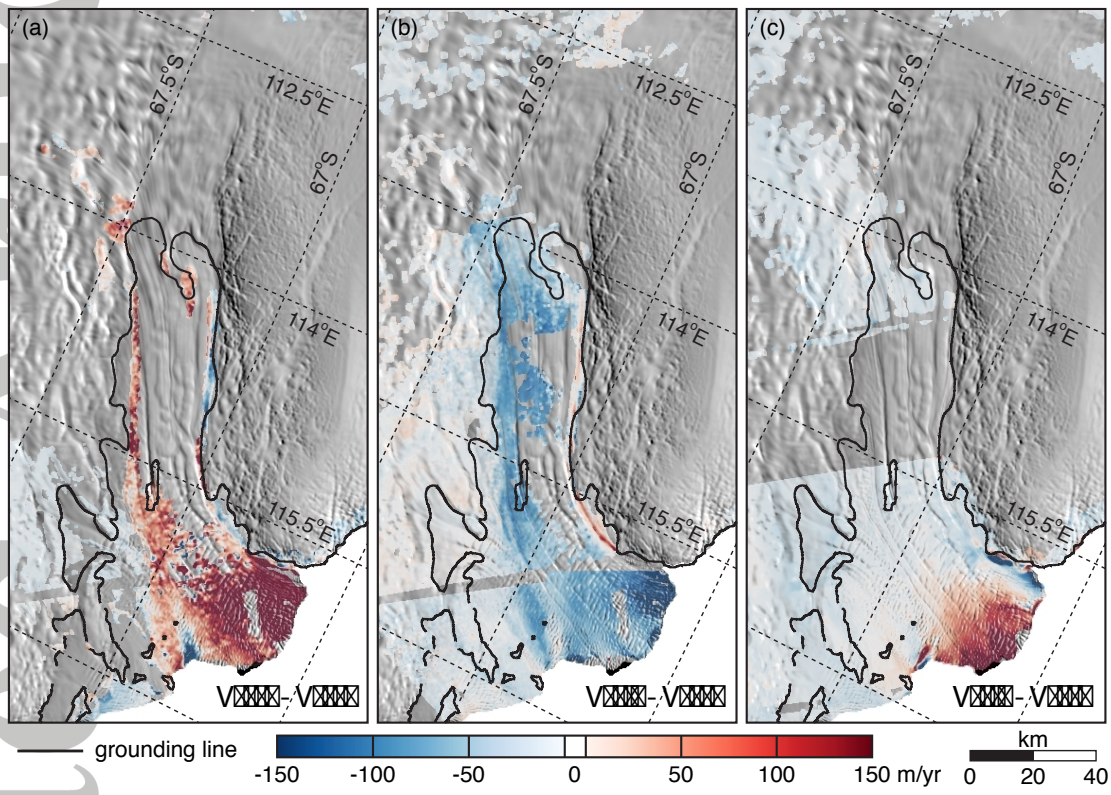

Figure 3. Change in flow speed from year (a) 2000 to 2007; (b) 2007 to 2013; and (c) 2009 to 2010 on Totten Glacier, East Antarctica, overlaid on a MODIS mosaic of Antarctica [*Scambos et al.*, 2007]. Grounding line from *Li et al.* [2015] is in black.